Characterization of six-bar spherical tensegrity lattice topologies

Alan Zhang*, Brian Cera, Alice Agogino

*University of California, Berkeley
Department of Mechanical Engineering, UC Berkeley
alanzhang89@berkeley.edu

Abstract

Tensegrity structures provide many key benefits such as their compliance, robustness, and high strength to weight ratio that are ideal for soft robotic applications. The Berkeley Emergent Space Tensegrities Laboratory, in collaboration with NASA Ames Research Center, is developing multiple six-bar spherical tensegrity robots to use as planetary landers and rovers. A new prototyping method uses a modular elastic lattice platform that serves as the tension network for the robot, allowing for multiple different shapes to be explored for the design of the robot. This paper explores different tensegrity lattice topologies and characterizes their effect on the impact resistance of the structure through a series of drop test experiments. The standard icosahedral "delta" lattice is simulated and tested to motivate new lattice topologies for hardware validation. We measure the accelerations experienced by a central payload carried by the robot and verify that the tensegrity structure does protect the payload from impact. Finally, the results are compared to provide insight in the design tradeoffs between the various lattice topologies.

Keywords: Tensegrity, elastic lattice, topology, impact resistance, deformation

1. Introduction

Tensegrity structures are mechanically robust assemblies of rigid bodies suspended in a tension network of elastic elements. First developed for art and architecture during the 1960s [1], [2], [3], [4], they have been used for a wide range of creative applications, such as dome structures [5], space structures [6], and origami nano-scale structures [7]. Recently, UC Berkeley worked with choreographer Jodi Lomask to help develop interactive (Figure 1a) and passive (Figure 1b) tensegrity structures in the Capacitor performance titled "Synaptic Motion", revolving around neuroscience and creativity [8], [9].

Figure 1a: Interactive tensegrity structures used in *Synaptic Motion* by Capacitor [8], [9]

Figure 1b: Suspended from the ceiling, a performer interacts with this tensegrity structure during *Synaptic Motion* by Capacitor © RJ Muna

Tensegrity structures have been of great interest in soft robotic applications due to their potential for robust locomotion [10]. Lightweight and compliant, they have an advantage in space applications where energy-efficiency and reliability are critical to mission success. In collaboration with the NASA Ames Research Center, the Berkeley Emergent Space Tensegrities Laboratory has been developing shape-shifting six-bar spherical tensegrity robots that can serve as both landers and rovers in a planetary exploration mission. The topology of our six-bar sphere-like robot is based on a tensegrity structure that consists of six rods and 24 cables. Each rod is connected to four cables to create a structure with eight equilateral triangles and 12 isosceles triangles, which are formed by the position of the rod ends. As not all nodes are connected by cables, each of the 12 isosceles triangles are referred to as open triangles with cable connecting two of its three edges. The eight equilateral triangles are referred to as closed triangles with cables connecting all three edges.

Prior work has focused on design and control using series-elastic actuation on a standard icosahedron delta geometry, where each tensile element consists of a cable and spring tied together [10], [11]. In contrast, using a modular tensegrity prototyping platform that replaces all the tensile elements with a single elastic lattice [12], we are now capable of rapidly testing the effects of new lattice topologies (Figure 2) on the locomotion behavior and impact resistance of the tensegrity structure.
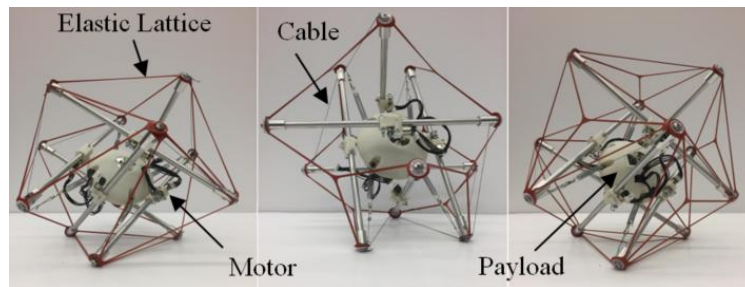

Figure 2: Six-bar tensegrity lattice topologies. From left to right: delta, Y-star, and hybrid lattice structures

The robots' current locomotion scheme uses motors to alter the cable lengths and deform the structure, allowing the robot to perform a "punctuated rolling" motion through controlled shape-shifting [13]. For faster and more efficient movement, the robot benefits from the additional compliance provided by a lower stiffness lattice. However, in a planetary exploration mission, the robot must also be able to survive drops from its initial deployment as well as subsequent landings from rolling down hills or craters. A higher stiffness lattice reduces the deformation experienced during an impact scenario, allowing the rods to absorb a greater portion of the kinetic energy through elastic buckling [14] and thus protecting the payload. The new tensegrity lattice topologies seek to balance this tradeoff between speed and robustness, and characterize the trade space of six-bar tensegrity robot structures.

2. Methods

The delta lattice topology's behavior is simulated in the NASA Tensegrity Robotics Toolkit (NTRT) [15] and all lattices are evaluated through hardware experiments. From the NTRT simulations we measure the robot's accelerations during a landing event. In hardware, we attach a Teensy 3.5 microprocessor at the central payload that logs data from an Adafruit ADXL377 accelerometer onto an SD card. The impact resistance of the structure is characterized by the maximum measured acceleration magnitude, which shows how effectively and reliably the structure protects the payload across different landing conditions. The results are compared to a base case of dropping a solid block of the same mass as the robot in order to quantify the effects of the tensegrity structure. For each topology, we parametrically sweep through lattice stiffness, drop heights, and robot orientations. We choose to drop the robot onto a closed triangle face, as well as onto an open triangle face with two rods landing perpendicular to the ground (Figure 3). The closed base triangle is the starting orientation needed for locomotion, while the open face triangle corresponds to a worst case scenario for the rod buckling on impact.
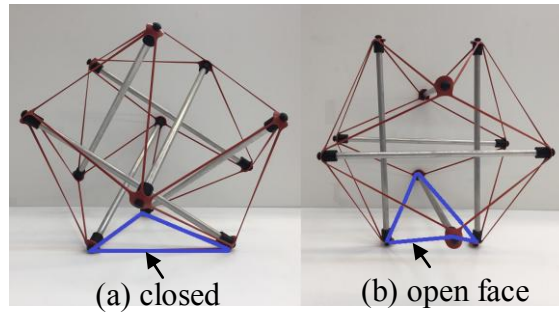
(a) closed   (b) open face

Figure 3: Tensegrity robot landing onto base triangle (a) and onto bars (b)

The physical parameters of the robot are found below in Table 1.

Table 1: Physical parameters of the tensegrity robot

Total mass	387 g
Rod mass	19.85 g
Rod length	30.48 cm (1 ft)
Lattice stiffness (single)	493 N/m
Lattice stiffness (double)	986 N/m

3. Results and Discussion

3.1. Simulations

To demonstrate the tensegrity concept's effectiveness in protecting a centrally-located payload, we utilized NTRT to evaluate the impact-resilience of the delta lattice topology with 986 N/m stiffness [12] and the model parameters given in Table 1 above. The lattice stiffness refers to a single length of lattice material, not the "effective stiffness" of the structure. Dropping the structure from heights of 1 m, 5 m, and 10 m in simulation under both landing orientations (open triangle or closed triangle), we record linear velocities of the system and take a finite-difference approximation, while using a Savitzky-Golay filter with frame size $n = 7$ (0.007 seconds) and 3rd-order polynomial fit to reduce noise in the data. Acceleration magnitudes in $G's$ ($1\ G\ =\ 9.8\ m/s^2$) exerted on the payload under drops from varying initial conditions are shown in Figure 4.
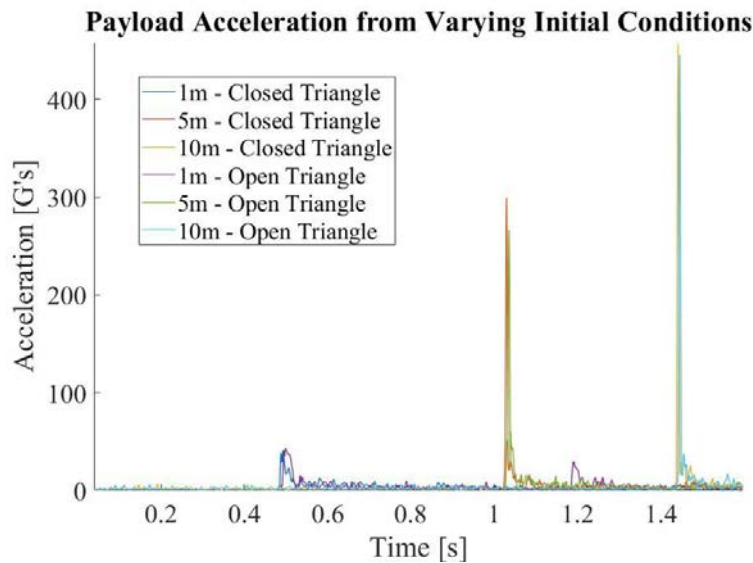

Figure 4: Results from simulated drop tests using the traditional delta elastic lattice topology with 986 N/m

From the results with this idealized model, we show that overall, the compliant structure causes the center capsule to observe lower magnitude accelerations in general (Figure 5). In comparison to the combined average acceleration felt by the individual rods at any given time, the payload is subject to acceleration magnitudes that are half (or less) than those felt by the rest of the structure during dynamic motion. The exception to this being the very large peaks at 1.0 s and 2.1 s, which are when the payload makes direct contact with the ground. With these results in hand, we moved ahead to hardware validation to test the delta topology as well as two novel elastic lattice geometries – "Y-star" and "hybrid" lattices.

5 m Simulated Drop Test Results, Open-Triangle

Legend:
- Payload Accel. - 493 N/m Stiffness
- Rod Accel. - 493 N/m Stiffness
- Max Payload Accel. - 493 N/m Stiffness
- Max Rod Accel. - 493 N/m Stiffness
- Payload Accel. - 986 N/m Stiffness
- Rod Accel. - 986 N/m Stiffness
- Max Payload Accel. - 986 N/m Stiffness
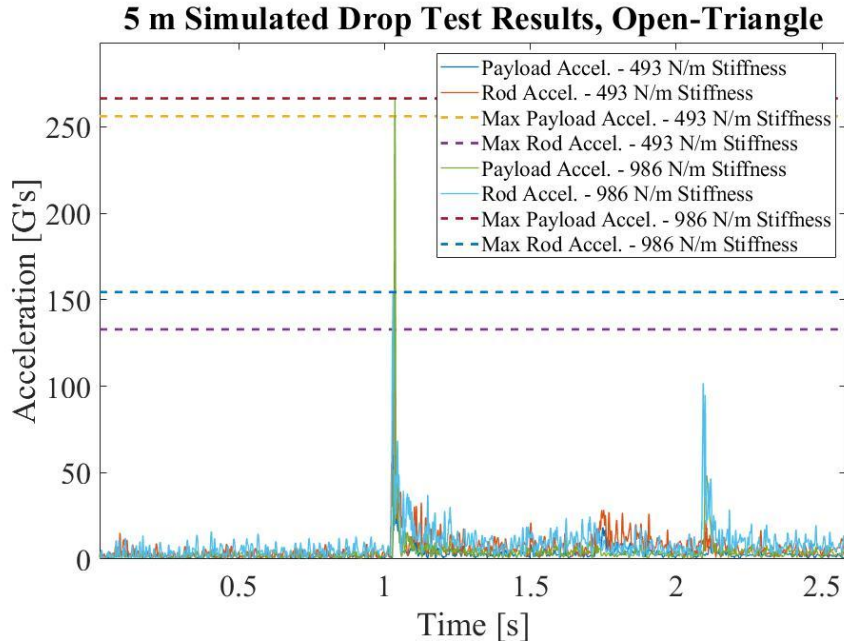- Max Rod Accel. - 986 N/m Stiffness

Figure 5: Drop test simulation results from 5 m with the delta lattice and different stiffness parameters

3.2 Drop Test Experiments

A summary of the peak acceleration magnitude for each drop test is found below in Table 2.

Table 2: Drop test results - maximum acceleration magnitudes

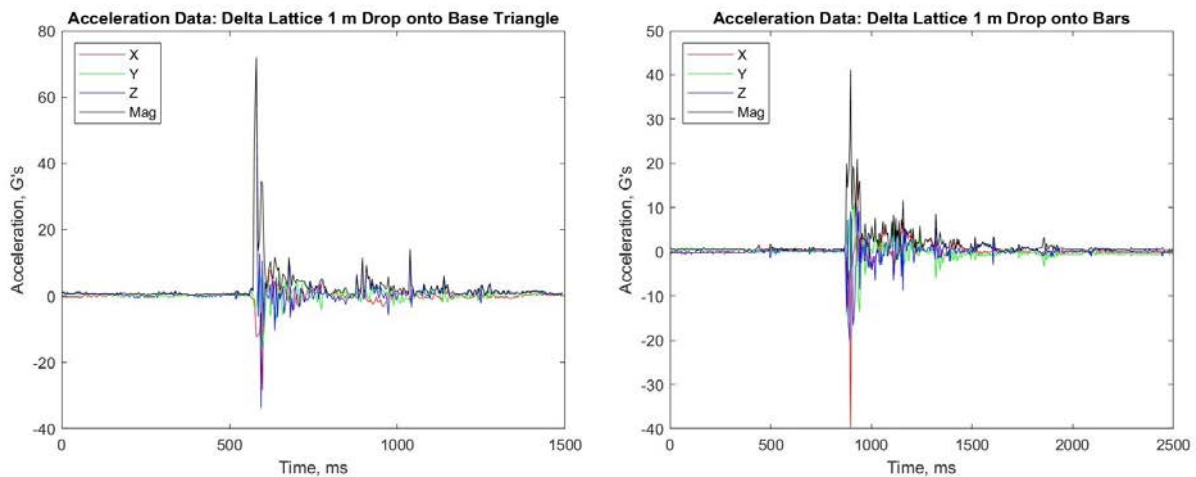| Topology	1 m Drop (G's)	5 m Drop (G's)
Base case: solid block	114.9	228.0
Y-star, closed face	82.8	-
Y-star, open face	42.9	-
Delta, closed face	59.0	-
Delta, open face	46.5	-
Hybrid, closed face	57.6	-
Hybrid, open face	40.9	-
Delta (double stiffness), closed face	47.6	175.1
Delta (double stiffness), open face	39.0	131.0
Hybrid (double stiffness), closed face	45.9	194.7
Hybrid (double stiffness), open face	38.1	157.8

Figure 6: Representative drop test acceleration data

Representative plots of acceleration data are shown above in Figure 6. During the tests, the central payload of sensors, actuators, motors and batteries (Figure 2) was observed to occasionally contact the rods of the robot, leading to an increase in the peak acceleration. This is due to the relative size of the payload in comparison to the tensegrity structure. The lower stiffness lattices were much more likely to contact the rods, so as a safety precaution they were removed from the 5 m drop tests. We also note that doubling the stiffness of the lattice reduced the peak acceleration, as expected, since the payload was less likely to contact the rods. Simulation results suggested that the stiffer lattices should experience higher peak payload accelerations, but this was not the case for our experiments due to the complex interactions created from the rod contact. The experimental data from the 1 m drops was approximately in the expected range of values according to simulation results. However, at 5 m the measured peak accelerations differed from the simulations to a greater extent, possibly due to a number of factors such as model parameter mismatch and simplified simulation dynamics.

The robot experienced significantly more deformation when landing on an open face, compressing to approximately half of its original height. In this mode the hybrid and delta lattices have comparable success in protecting the payload. When two rod ends move apart, that motion is contained within the strain of the lattice because the lattice is in line with the direction of motion. However, in the Y-star lattice, the same motion causes rotation between two prongs of the Y shape as well. This causes the Y-star lattice to have the most deformation upon impact, and makes the payload more vulnerable to impact. When landing on the bars, there is no observable difference between the lattices. Most of the impact energy is absorbed by the bars during the initial landing and then by the structure during subsequent bouncing and rolling, so the payload experiences less instantaneous acceleration as a result. In all tests, the robot experienced less acceleration than the base case of undamped impact.

4. Conclusions and Recommendations

Three different modular tensegrity lattice systems were tested in drop test experiments to evaluate their impact resistance characteristics. The tensegrity systems were shown to reduce the maximum acceleration experienced during a landing event. However, the lattice alone is not sufficient as a structural solution, and other impact dampening mechanisms such as sacrificial struts should be considered. Orienting the robot to land on two vertical bars shows the most promise in protecting the payload, and since the lattice has less effect in this landing orientation we may be able to decouple the two problems of locomotion speed and impact resistance.

While all tests demonstrated the benefits of the tensegrity structure for payload protection, there are several improvements we can make to our system before continuing with further drop tests. By scaling up the rod lengths we can make more room for the payload in the center of the structure to reduce the force associated with contact with the rods or ground during impact and to ensure that we are only

measuring the effects of the lattice. A new design for the elastic elements of the tensegrity structure could use a new material such as latex tubing or a mechanism such as progressive stage springs. Both of these options are strain-stiffening and could provide the elastic compliance required for locomotion and the small deformations that cushion the payload during an impact. Then, when the elastic element reaches a critical strain value it will become much harder to deform the structure and will prevent the payload from making contact with the rods or ground. Additionally, the accelerometer sensor can be streamlined to reduce data logging overhead, thereby improving the frequency response and data capture rate. This will help improve our statistical measurements, as we are never certain when we may be missing peak accelerations during the drop.

In addition to the improvements mentioned above, future work could include modeling the walking behavior as a function of lattice properties and also designing robust rods and a mechanism to rotate the robot while it is falling to consistently land on two vertical rods. Collectively, these results will inform future decisions in developing novel structural designs and control policies for these versatile robots.

Acknowledgements

References

[1] K. Snelson, "Continuous tension, discontinuous compression structures," U.S. Patent 3 169 611, 1965.

[2] B. Fuller, " Tensegrity," Portfolio and Art News Annual, Vol. 4, Art Foundation Press, Inc., New York, pp. 112–127, 1961.

[3] K. Snelson, " Kenneth Snelson, Art and Ideas," Kenneth Snelson, Marlborough Gallery, NY, 2013. http://kennethsnelson.net/KennethSnelson_Art_And_Ideas.pdf. [Accessed Apr. 2018].

[4] C.R. Calladine, Buckminster Fuller's "tensegrity" structures and Clerk Maxwell's rules for the construction of stiff frames. *International Journal of Solids and Structures*, *14*(2), 1978, pp. 161-172.

[5] F. Feng, " Structural Behavior of Design Methods of Tensegrity Domes," J. Constr. Steel Res., 61(1), 2005, pp. 22–35.

[6] A.G. Tibert, S. Pellegrino, "Review of form-finding methods for tensegrity structures," *International Journal of Space Structures*, *26*(3), 2011, pp. 241-255.

[7] B. Saccà, C.M. Niemeyer, "DNA origami: the art of folding DNA", *Angewandte Chemie International Edition*, *51*(1), 2012, 58-66.

[8] A.M. Agogino, "Synaptic Motion: Colin Ho Designs Tensegrity-Inspired Dance Apparatus," UC Berkeley, 2014. http://best.berkeley.edu/2014/09/19/synaptic-motion-colin-ho-designs-tensegrity-inspired-dance-apparatus/. [Accessed Apr. 2018].

[9] Capacitor, Synaptic Motion, 2014. https://www.capacitor.org/synaptic-motion/. [Accessed Apr. 2018].

[10] K. Caluwaerts, J. Despraz, A. Iscen, A. P. Sabelhaus, J. Bruce, B. Schrauwen, and V. SunSpiral, "Design and control of compliant tensegrity robots through simulation and hardware validation," *Journal of The Royal Society Interface*, vol. 11, no. 98, pp. 20140520-20140520, 7 2014. [Online]. Available: http://rsif.royalsocietypublishing.org/content/11/98/20140520. [Accessed Feb. 2018].

[11] L.H. Chen, K. Kim, E. Tang, K. Li, R. House, E. Zhu, ... & E. Jung, "Soft spherical tensegrity robot design using rod-centered actuation and control," *Journal of Mechanisms and Robotics*, *9*(2), 025001, 2017.

[12] L.-H. Chen, M. Daly, A. P. Sabelhaus, L. A. Janse van Vuuren, H. Garner, et al. "Modular Elastic Lattice Platform for Rapid Prototyping of Tensegrity Robots," in *Proceedings of the ASME 2017 International Design Engineering Technical Conferences and Computers and Information in Engineering Conference, IDETC/CIE 2017: 41st Mechanisms and Robotics Conference, Cleveland, Ohio, USA, August 6-9, 2017.*

[13] K. Kim, A. K. Agogino, A. Toghyan, D. Moon, L. Taneja, and A. M. Agogino, "Robust learning of tensegrity robot control for locomotion through form-finding," in 2015 IEEE/RSJ International Conference on Intelligent Robots and Systems (IROS). IEEE, 9 2015, pp. 5825-5831. [Online]. Available: http://ieeexplore.ieee.org/lpdocs/epic03/wrapper.htm?arnumber=7354204. [Accessed Feb. 2018].

[14] J. Rimoli. "On the impact tolerance of tensegrity-based planetary landers," in 57th AIAA/ASCE/AHS/ASC Structures, Structural Dynamics, and Materials Conference, San Deigo, California, USA, January 4-8, 2016.

[15] NASA tensegrity robotics toolkit. [Online]. https://ti.arc.nasa.gov/tech/asr/groups/intelligent-robotics/tensegrity/NTRT/. [Accessed Apr. 2018].